
HOKKAIDO UNIVERSITY

Title	Coral Ba/Ca Analysis Using ICP-OES With an Ultrasonic Nebulizer
Author(s)	Watanabe, Takaaki K.; Watanabe, Tsuyoshi; Ohmori, Kazuto; Yamazaki, Atsuko
Citation	Geochemistry geophysics geosystems, 22(8), e2021GC009646 https://doi.org/10.1029/2021GC009646
Issue Date	2021-08-01
Doc URL	http://hdl.handle.net/2115/83968
Rights	An edited version of this paper was published by AGU. Copyright 2021 American Geophysical Union.
Type	article
File Information	Geochem. Geophys. Geosyst.22-8_e2021GC009646.pdf


Instructions for use

Hokkaido University Collection of Scholarly and Academic Papers : HUSCAP

Geochemistry, Geophysics, Geosystems

TECHNICAL REPORTS: METHODS
10.1029/2021GC009646

Key Points:

- A new analytical method for (Ba/Ca) in coral skeletons using ICP-OES and an ultrasonic nebulizer
- An ultrasonic nebulizer enhances signals for trace element analyses in coral skeleton
- Ba/Ca is obtained by applying the intensity ratio calibration method and analyzing at a certain Ca concentration

Supporting Information:

Supporting Information may be found in the online version of this article.

Correspondence to:

T. Watanabe,
nabe@sci.hokudai.ac.jp

Citation:

Watanabe, T. K., Watanabe, T., Ohmori, K., & Yamazaki, A. (2021). Coral Ba/Ca analysis using ICP-OES with an ultrasonic nebulizer. *Geochemistry, Geophysics, Geosystems*, *22*, e2021GC009646. https://doi.org/10.1029/2021GC009646

Received 12 JAN 2021
Accepted 1 JUL 2021

© 2021. American Geophysical Union. All Rights Reserved.

Coral Ba/Ca Analysis Using ICP-OES With an Ultrasonic Nebulizer

Takaaki K. Watanabe[1], Tsuyoshi Watanabe[1,2,3], Kazuto Ohmori[1,4], and Atsuko Yamazaki[1,2,5]

[1]Department of Natural History Sciences, Faculty of Science, Hokkaido University, Sapporo, Japan, [2]KIKAI Institute for Coral Reef Sciences, Kagoshima, Japan, [3]Research Institute for Humanity and Nature, Kyoto, Japan, [4]Hokkaido Research Organization, Research Institute of Energy, Environment and Geology, Sapporo, Japan, [5]Department of Earth and Planetary Sciences, Faculty of Science, Kyusyu University, Fukuoka, Japan

Abstract The barium/calcium ratio (Ba/Ca) in coral skeletons has been used as a proxy to understand river floods and oceanic upwelling in the tropics and subtropics for the past centuries. Here, we establish a new method for Ba/Ca analysis using inductively coupled plasma optical emission spectrometry (ICP-OES), which has been widely used for coral proxy analyses and can save analysis time compared to other methods. We analyze Ba/Ca by combining an ultrasonic nebulizer with the intensity ratio calibration method to improve the signal intensity of Ba. Our method can determine Ba/Ca in samples with a Ca concentration of 9 mg/L with excellent analytical precision (<0.17 μmol/mol) using ICP-OES.

1. Introduction

Massive coral skeletons (e.g., *Porites* sp.) inhabiting tropical and subtropical oceans provide a century-long archive of marine environmental changes based on the composition of trace elements (TEs) in their aragonite skeletons (Hendy et al., 2002; McCulloch et al., 2003; Thompson et al., 2015; Zinke et al., 2004). The ratio of barium per calcium (Ba/Ca) in coral skeleton reflects Ba concentrations in the sea surface (Gonneea et al., 2017; LaVigne et al., 2016; Lea et al., 1989; Montaggioni et al., 2006; Yamazaki et al., 2020). Ba concentrations in the sea surface are increased by the input of river water and by disorbed from suspended particles (Bryan et al., 2019; Weldeab et al., 2007). Since the Ba concentration in seawater is higher in the deep sea than the sea surface (similar to the distribution of nutrients), upwelling increases the Ba concentration in the sea surface. Ba/Ca has been used as an indicator for river runoff (Ito et al., 2020; McCulloch et al., 2003; Phan et al., 2019; Sowa et al., 2014; Yu et al., 2015), dust storms (Bryan et al., 2019), and upwelling (Tudhope et al., 1996).

Coral Ba/Ca has been analyzed using the expensive instrument (e.g., thermal ionization mass spectrometry (TIMS) and inductively coupled plasma mass spectrometry (ICP-MS); Bryan et al., 2019; Gonneea et al., 2017; LaVigne et al., 2016; Montaggioni et al., 2006; Tudhope et al., 1996). Inductively coupled plasma optical emission spectrometry (ICP-OES), which has been widely used for coral strontium per calcium ratio (Sr/Ca) analyses, could provide the trace element per calcium ratio (TE/Ca) in coral skeletons (Schrag, 1999; T. Watanabe et al., 2001; T. K. Watanabe et al., 2020; Zinke et al., 2004). ICP-OES has the advantage of the low running cost and high time-efficiency of analysis, making this instrument suitable for establishing a century-long record of coral proxy (Cantarero et al., 2017; Schrag, 1999; T. K. Watanabe et al., 2020). However, TE/Ca analyses using ICP-OES are often complicated because high Ca concentrations in coral skeletons might interfere with the TE analysis. Cantarero et al. (2017) established an analytical method for Ba/Ca using the double viewing system of ICP-OES. They analyzed the Ba concentrations using the axial torch view. They avoided Ca oversaturation using the less sensitive radial torch view (Cantarero et al., 2017). In their method, the matrix interferences in Ba/Ca were corrected by linear regression between analytical results of the standard solutions with different Ca concentrations (10–55 mg/L) and a specific value of Ba/Ca.

Here, we introduce a new analytical method for coral Ba/Ca combining an ultrasonic nebulizer with ICP-OES. The ultrasonic nebulizer system composed of a piezoelectric transducer and a desolvation system has the advantage of signal enhancement (Olson et al., 1977). The sample solutions are introduced to the piezoelectric transducer on the ultrasonic nebulizer and converted to aerosols from solutions. The desolvation via heating/cooling concentrates the aerosol and uniforms its size. Enhancing the analytical signals is obtained by improvement in transport efficiency of the aerosols uniformed their size and concentrated. The

15252027, 2021, 22, Downloaded from https://agupubs.onlinelibrary.wiley.com. By Hokkaido University- on [04/10/2021]. Re-use and distribution is strictly not permitted, except for Open Access articles

15252027, 2021, 22, Downloaded from https://agupubs.onlinelibrary.wiley.com By Hokkaido University - on [04/10/2021]. Re-use and distribution is strictly not permitted, except for Open Access articles

enhanced signal allows us to analyze TE at low concentrations or in small sample amounts with better reproducibility. However, the Ca signal in coral skeletons is possibly oversaturated and interferes with the TE analysis by using the ultrasonic nebulizer because Ca is an easily ionized element and contained at a high concentration in the coral skeleton. We apply the intensity ratio calibration method (de Villiers et al., 2002) to Ba/Ca analysis. In this method, a regression line is established between the ratios of TE intensity per Ca intensity (i.e., intensity ratios) and TE/Ca in the calibration solutions. The TE/Ca is directly obtained from the intensity ratio in sample solutions owing to the regression line. This calibration method has the potential to improve the uncertainty of calibration by avoiding the effect of high Ca concentration on TE analyses in the calibration solution.

2. Method

2.1. Instrumental Conditions and Settings

We used an ultrasonic nebulizer (U-5000AT+, Teledyne CETAC Technologies) and an autosampler (ASX-260, Teledyne CETAC Technologies) attached to ICP-OES (iCAP 6200, Thermo Scientific). Our ICP-OES setting was shown in Table S1. The solutions (samples and standards) were introduced by the autosampler and the ultrasonic nebulizer to ICP. We rinsed the whole analytical line from the autosampler to the torch using 6% HNO_3 solutions following each sample injection to avoid contamination between the samples and to decrease the memory effect. The temperature at heating and cooling tube for desolvation on the ultrasonic nebulizer were set at 140 °C and 4 °C, respectively. We washed the chamber and heating/cooling tube on the ultrasonic nebulizer by filling 6% HNO_3 for one day and rinsed with ultrapure water (18.2 MΩ-cm at 25 °C, Millipore) every week. We appropriately washed labware for our analysis. We conducted soak washing for all plastic labware in order of (1) neutral detergent, (2) HNO_3, (3) HCl, and (4) deionized water. Plastic labware was put in each bath for one day, and it was rinsed with deionized water before transferring to the next bath. Plastic labware was rinsed with ultrapure water after putting it in the deionized water bath for one day, and then it was dried on the shelf under a high-efficiency particulate air (HEPA) filtered environment.

2.2. Evaluations of Stability Against the Selection of Wavelength and Ca Concentration

The Ca wavelength for our method was determined by evaluating the stability of TE/Ca in the standard solutions at different Ca wavelengths and various Ca concentrations. We analyzed the TE/Ca of JCp-1 solutions (international standard for TE in coral skeletons, made from the *Porites* skeleton; Okai et al., 2002) with 12 different Ca concentrations (range of Ca concentration: 3–25 mg/L). JCp-1 (n = 12; 0.39–3.3 mg) was dissolved in 50 mL of 3% HNO_3 acid and diluted to the target concentrations of Ca. 3% HNO_3 acid was used as the blank solution (n = 5). This evaluation was carried out with four ionic lines of Ca (318.1, 315.8 370.6, and 373.6 nm) by the axial view. We used the intense ionic line of Ba (455.4 nm) and the relatively weak line of Sr (346.4 nm) by the axial view not to diminish the Ba signal and to avoid the oversaturation of Sr. The solutions of each Ca concentration were analyzed three times (i.e., n = 36). We calculated the intensity ratios and the offset of TE/Ca (Sr/Ca and Ba/Ca) for the stability test using the following equations:

$$IR = \frac{SI_{\mathrm{TE}} - BI_{\mathrm{TE}}}{SI_{\mathrm{Ca}} - BI_{\mathrm{Ca}}}$$

$$F = \frac{(IR)}{(\mathrm{TE}_{\mathrm{con}})}$$

where IR is the intensity ratio, SI_{TE} is the TE intensity in the solution, SI_{Ca} is the Ca intensity in the solution, BI_{TE} is the TE intensity in the blank solution, BI_{Ca} is the Ca intensity in the blank solution, F is the offset, intensity ratio relative to the consensus value of TE/Ca in JCp-1 (TE_{cer}, Ba/Ca: 7.465 μmol/mol; Sr/Ca: 8.838 mmol/mol; Hathorne, Gagnon, et al., 2013). We reported the offset as a normalized value relative to that at a Ca concentration of 20 mg/L. The intensity ratio and offset were estimated using our considered wavelength of Ba, Sr, and Ca. We compared the analytical results of the JCp-1 solution using the ultrasonic

15252027, 2021, 22, Downloaded from https://agupubs.onlinelibrary.wiley.com. By Hokkaido University- on [04/10/2021]. Re-use and distribution is strictly not permitted, except for Open Access articles

nebulizer with using the pneumatic nebulizer. The results of JCp-1 at different Ca concentrations using the pneumatic nebulizer were introduced in T. K. Watanabe et al. (2020).

2.3. Analytical Protocol

2.3.1. Solutions for Calibration Standards and Samples

We prepared six solutions containing different concentrations of TEs and constant Ca concentrations for the intensity ratio calibration method. We weighed and mixed element standard solutions (i.e., calibration solutions; Ca, Sr, and Ba; FUJIFILM WAKO Pure Chemical Corporation) using a balance (BP 211D, Sartorius; reproducibility: <±0.05 mg; Table S2). Then, mixed standard solutions were gravimetrically diluted to a Ca concentration of 9 mg/L with ultrapure water. We calculated TE/Ca in the calibration solutions based on the weighing results of the element standard solutions. The ranges of Ba/Ca and Sr/Ca in the calibration solutions (Ba/Ca: 0–12 μmol/mol; Sr/Ca: 0–9.8 mmol/mol) overlapped the reported ranges of coral TE/Ca (Ba/Ca: ca. 4–10 μmol/mol, LaVigne et al., 2016; Sr/Ca: ca. 8.5–9.5 mmol/mol, DeCarlo et al., 2016). Weighed coral powders (120 ± 20 μg, as samples) and JCp-1 (as running standards) were dissolved in 25% HNO_3 acid and then diluted to a Ca concentration of 9 mg/L and 3% HNO_3 with ultrapure water.

2.3.2. Sample Analyses

We used the ionic lines of Ba (455.4 nm), Sr (346.4 nm), and Ca (318.1 nm) for our method. The calibration solutions were analyzed prior to every sequence (including samples, running standards, and blanks). We established a regression line based on the intensity ratio and the estimated TE/Ca in the calibration solutions. The TE intensities in the calibration solutions were positively correlated with the calculated TE/Ca (Ba: $r > 0.99$; $p < 0.01$; $n = 6$; Sr: $r > 0.99$; $p < 0.01$; $n = 6$), while the Ca intensity was constant (Figures 1a and 1b, Table S3). In both Ba/Ca and Sr/Ca, the intensity ratios were significantly correlated with the calculated values (Ba/Ca: $r > 0.999$; $p < 0.01$; $n = 6$; Sr/Ca: $r > 0.999$; $p < 0.01$; $n = 6$; Figures 1c and 1d). We tested the stability of the calibration by estimating the offset of the intensity ratio in calibration solutions relative to their known TE/Ca values as the following equation:

$$F = \frac{IR}{\mathrm{TE}_{\mathrm{calib}}}$$

where IR is the intensity ratio (Table S3), $\mathrm{TE}_{\mathrm{calib}}$ is the known value of TE/Ca in the calibration solutions (Table S2), F is the offset. We reported the offset as the normalized value relative to that at 8.86 mmol/mol or 7.94 μmol/mol (Table S2). TE/Ca in samples and running standards were calculated from their intensity ratios using the regression line derived from the analytical result of the calibration. Running standards were analyzed for the first three samples and after every five sample measurements in a sequence. According to the analytical results of the running standards, we corrected the instrumental drift and the difference in absolute value in each sequence. The instrumental drift in TE/Ca was detrended by referring to a best-fit curve between analysis times and TE/Ca in the running standards (see T. K. Watanabe et al., 2020).

2.4. Verification of Precision and Accuracy

The analytical precision and accuracy of our method were verified using the analytical results of JCp-1 ($n = 545$) and JCt-1 ($n = 13$; the international standard for TE in bivalve shells, made from *Tridacna* shell; Okai et al., 2002). The JCp-1 data set was compiled from the results analyzed by our method. The JCp-1 data set contained running standards ($n = 525$; 31 sequences) and the result of the replicate measurements ($n = 20$). JCt-1 solutions were analyzed using the same method as JCp-1. For accuracy verification, we calculated differences in TE/Ca between the means of the values (our JCt-1 and JCp-1 data sets) prior to corrections for instrumental drift or the results of the interlaboratory works (Hathorne, Gagnon, et al., 2013) and the consensus values (Hathorne, Gagnon, et al., 2013), following equation:

$$D = \frac{\left(\mathrm{TE}_{\mathrm{con}} - \mathrm{TE}\right)}{\left(\mathrm{TE}_{\mathrm{con}}\right)} \times 100$$

where D is the difference, $\mathrm{TE}_{\mathrm{con}}$ is the consensus value of TE/Ca in JCp-1 or JCt-1, and TE is TE/Ca in JCp-1 or JCt-1 of our data set or the results of the interlaboratory work. The consensus values of Ba/Ca in JCp-1

15252027, 2021, 22, Downloaded from https://agupubs.onlinelibrary.wiley.com. By Hokkaido University- on [04/10/2021]. Re-use and distribution is strictly not permitted, except for Open Access articles

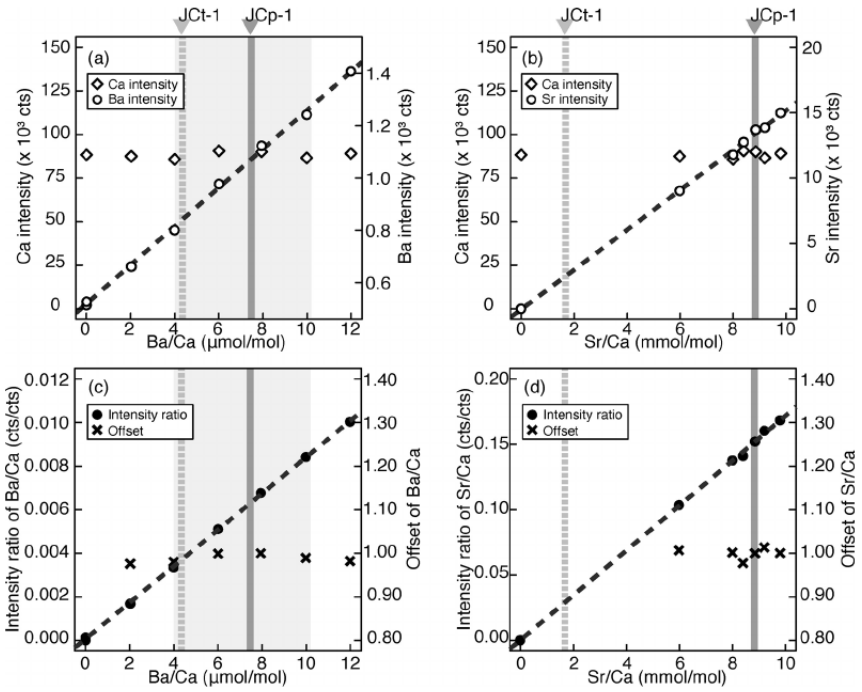

Figure 1. Analytical results of calibration solutions at a Cawavelength of 318.1 nm. (a) and (b) plots of the TE/Ca and intensity. The open circles and diamonds indicate TE and Ca intensity, respectively. The composition of the calibration solutions and the analytical result is shown in Tables S2 and S3. (c) and (d) relationships among the intensity ratio of TE/Ca, the offset of TE/Ca, and TE/Ca. The closed circles and cross plots indicate the intensity ratio of TE/Ca and the offset of TE/Ca, respectively. The gray solid and dashed lines indicate the consensus values of JCp-1 and JCt-1 (Hathorne, Gagnon, et al., 2013). The gray hatched areas indicate the reported variable range of coral Ba/Ca (LaVigne et al., 2016).

and JCt-1 with their standard deviations were 7.465 ± 0.655 and 4.348 ± 0.280 μmol/mol, respectively. The consensus values of Sr/Ca in JCp-1 and JCt-1 with their standard deviations were 8.838 ± 0.042 and 1.680 ± 0.026 mmol/mol, respectively (Hathorne, Gagnon, et al., 2013). The 95% confidence ellipses of interlaboratory works were calculated using the free software R (R core team, 2020). The precision was verified based on our JCp-1 data set after correcting the instrumental drift and the mean difference in each sequence.

3. Results

3.1. Stability Evaluations

We analyzed 36 solutions of JCp-1 with 12 Ca concentrations (3–25 mg/L) using the ultrasonic nebulizer. Ranges of the Ba (Sr) intensity of JCp-1 were 654–1,566 cts (3,095–27,234 cts) using the ultrasonic nebulizer. The averaged value of Ba (Sr) intensity in blank was 496 ± 12 cts (−24 ± 4 cts; 1 SD) using the ultrasonic nebulizer (Figures 2a and 2b). We compared with the analytical results of 90 solutions of JCp-1 with 17 Ca concentrations (3–25 mg/L) using the pneumatic nebulizer. The range of the Ba (Sr) intensity using the pneumatic nebulizer was 888–1,163 cts (882–7,652 cts; Figures 2a and 2b). The averaged value of Ba (Sr) intensity in blank was 884 ± 32 cts (−2 ± 3 cts; 1 SD). The Ba (Sr) intensities using the ultrasonic nebulizer were 4.2–6.0 (3.5–3.7) times higher than those using the pneumatic nebulizer. The blank of Ba intensity using the ultrasonic nebulizer was 44% lower than that using the pneumatic nebulizer.

15252027, 2021, 22, Downloaded from https://agupubs.onlinelibrary.wiley.com. By Hokkaido University- on [04/10/2021]. Re-use and distribution is strictly not permitted, except for Open Access articles

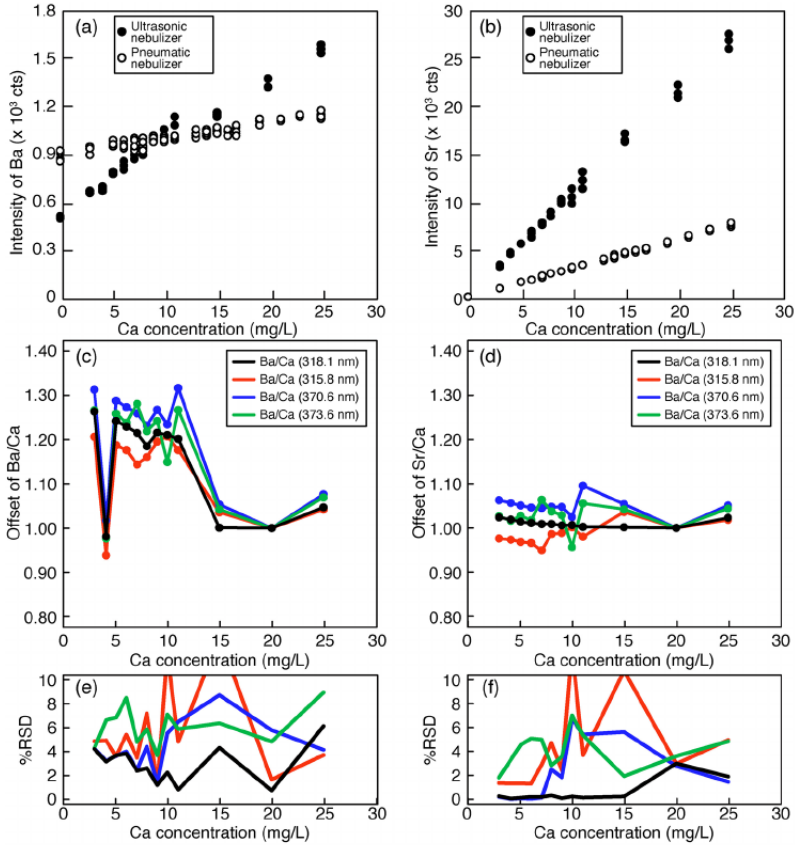

Figure 2. The stability of Ba/Ca and Sr/Ca in JCp-1 for the ultrasonic nebulizer. (a) and (b) the signal intensity of Ba (455.4 nm) and of Sr (346.4 nm) in JCp-1 solutions using the ultrasonic nebulizer (closed circles) and the pneumatic nebulizer (open circles). (c) and (d) the offset relative to the consensus value of Ba/Ca and Sr/Ca in JCp-1 using the ultrasonic nebulizer. The black, red, blue, and green lines indicate Ca wavelength at 318.1, 315.8, 370.6, and 373.6 nm, respectively. (e) and (f) %RSD of Ba/Ca and Sr/Ca in JCp-1 using the ultrasonic nebulizer.

We calculated the offset of TE/Ca using JCp-1 solutions for our stability test and using the calibration solutions (Figures 1c, 1d, 2c and 2d). The offset of Ba/Ca in JCp-1 was stable at Ca concentrations of 9 ± 2 mg/L (at the Ca 318.1 nm; Figure 2c). The relative standard deviation (%RSD) of Ba/Ca at Ca concentrations of 9 ± 2 mg/L were from 0.83 to 2.62 (Figure 2e). The offsets of Sr/Ca were stable, at 318.1 nm wavelength below Ca concentration of 15 mg/L (Figure 2d). The %RSD of Sr/Ca below Ca concentrations of 15 mg/L were from 0.06 to 0.32 (Figure 2f). The offsets of TE/Ca in the calibration standard were stable in the calibration ranges, as they did not show any trend and anomalous values (Figures 1c and 1d).

3.2. Accuracy and Precision

The means of our Ba/Ca prior to corrections for instrumental drift were 6.88 ± 0.28 (n = 545; 1 SD; Figure 3a) and 4.04 ± 0.08 μmol/mol (n = 13; 1 SD; Figure S1a) in JCp-1 and JCt-1, respectively. The differences of Ba/Ca between the means of our values prior to corrections for instrumental drift and the consensus values were −7.89% and −7.05% in JCp-1 and JCt-1, respectively (Figure 4a). The differences of Ba/Ca between the interlaboratory work and the consensus values were −5.60%–18.29% in JCp-1 and −7.59%–13.57% in JCt-1

15252027, 2021, 22, Downloaded from https://agupubs.onlinelibrary.wiley.com. By Hokkaido University- on [04/10/2021]. Re-use and distribution is strictly not permitted, except for Open Access articles

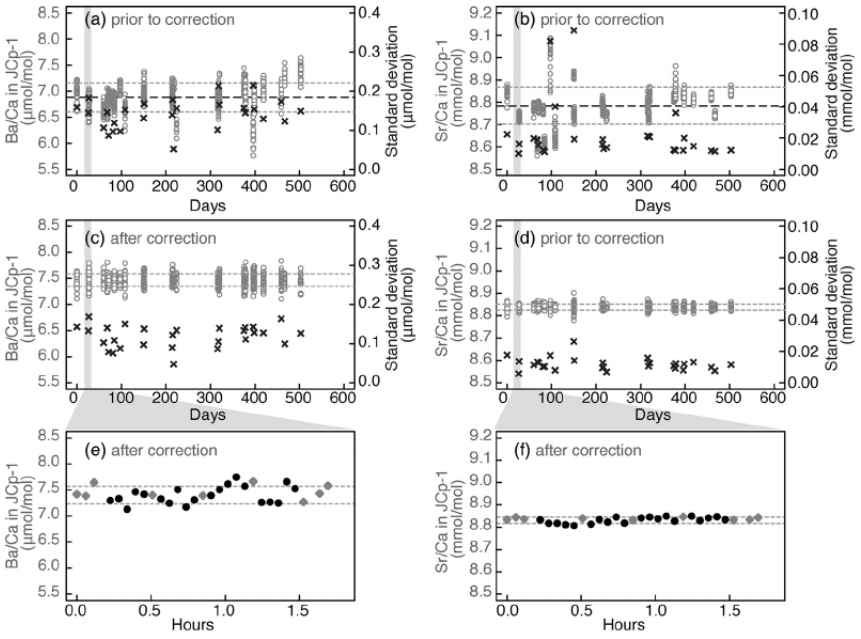

Figure 3. JCp-1 data set using our method. (a) and (b) values of TE/Ca prior to corrections for instrumental drift. Note that the instrumental drift is included. The black dashed lines show the mean values. The gray dashed lines show the variable range (1 SD). (c) and (d) values of TE/Ca after corrections for instrumental drift. The circles and crosses indicate TE/Ca and standard deviation (1 SD) in each sequence, respectively. The gray hatched areas on (a) to (d) correspond to the replicate measurements. (e) and (f) enlarged figures of the results in replicate measurements. The black circles and gray diamonds indicate the replicate samples and the running standards, respectively.

(Figure 4a). The means of Sr/Ca prior to corrections for instrumental drift were 8.785 ± 0.082 (n = 545; 1 SD; Figure 3b) and 1.624 ± 0.004 mmol/mol (n = 13; 1 SD; Figure S1b) in JCp-1 and JCt-1, respectively. The differences of Sr/Ca between the means of our values prior to corrections for instrumental drift and

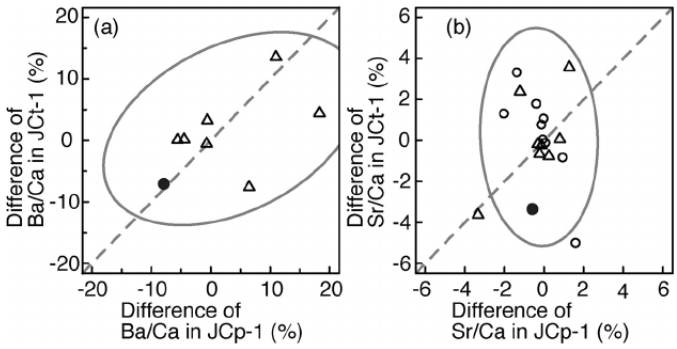

Figure 4. The differences of TE/Ca (a: Ba/Ca; b: Sr/Ca) in JCp-1 and JCt-1 between the means of our values prior to corrections for instrumental drift or the interlaboratory data and the consensus values (Hathorne, Gagnon, et al., 2013). The closed circles show the means of our values prior to corrections for instrumental drift. The open circles show the interlaboratory data using ICP-OES. The triangles show the interlaboratory data using ICP-MS. The gray dashed lines indicate 1:1 lines. The gray ellipses show the 95% confidence ellipse of the interlaboratory work.

15252027, 2021, 22, Downloaded from https://agupubs.onlinelibrary.wiley.com. By Hokkaido University- on [04/10/2021]. Re-use and distribution is strictly not permitted, except for Open Access articles

the consensus values were −0.60% and −3.35% in JCp-1 and JCt-1, respectively (Figure 4b). The differences of Sr/Ca between the interlaboratory work and the consensus values were −3.34%–1.58% in JCp-1 and −5.00%–3.57% in JCt-1 (Figure 4b). The differences between the means of our values prior to corrections for instrumental drift and the consensus value were within the confidence ellipse (Figure 4).

The standard deviations (1 SD) of Ba/Ca and Sr/Ca after corrections for instrumental drift were ±0.12 μmol/mol and ±0.013 mmol/mol, respectively ($n = 545$; 31 sequences; Figures 3c and 3d). The standard deviations (1 SD) of Ba/Ca and Sr/Ca values after corrections for instrumental drift in each sequence are from 0.05 to 0.17 μmol/mol and from 0.006 to 0.026 mmol/mol, respectively (Figures 3c and 3d). The standard deviations (1 SD) of the replicate measurements after the correction for instrumental drift were ±0.17 μmol/mol and ±0.014 mmol/mol for Ba/Ca and Sr/Ca, respectively ($n = 20$; Figures 3e and 3f).

4. Discussion

Applying the ultrasonic nebulizer to the ICP-OES helps us to enhance the signal intensity of the TE in coral skeletons (Figures 2a and 2b). The advantage of the ultrasonic nebulizer likely contributes to improving the detection limits compared to the pneumatic nebulizer. Our method using the ultrasonic nebulizer determines coral Ba/Ca and Sr/Ca with good analytical precisions (Ba/Ca: <±0.17 μmol/mol; Sr/Ca: <±0.026 mmol/mol), as inferred from the JCp-1 data set (Figures 3c and 3d) and the results of the replicate measurements (Figures 3e and 3f). TE/Ca analysis using ICP-OES is often hampered due to high Ca concentrations (Cantarero et al., 2017; de Villiers et al., 2002). The offsets of Ba/Ca largely change with the increase of Ca concentrations in our ultrasonic nebulizer system (Figure 2c). This implies that the Ba/Ca analyzed with the ultrasonic nebulizer is unstable with the increase of Ca concentration. The effect of high Ca concentration would be avoided by analyzing at a certain Ca concentration and applying the intensity ratio calibration method using a Ca wavelength of 318.1 nm (Figure 1). The constant concentration of Ca in the calibration and sample solutions would allow us to obtain Ba/Ca and Sr/Ca at the same sensitivity throughout the sequence (Figures 1 and 2). We decide that the target of Ca concentration in the calibration and sample solutions is 9 ± 2 mg/L because the offset of Ba/Ca and Sr/Ca are stable in our stability evaluation (Figures 1 and 2). The conventional calibration method is based on calibrating each element and obtaining TE/Ca from concentrations of the calibration-calculated element. This conventional method may influence the accuracy and precision of Ba/Ca analyses due to the matrix interference, and it is required matrix correction, as shown by Cantarero et al. (2017).

Our method provides coral Ba/Ca with little bias in a wide range of Ba/Ca values, as shown by comparing the JCp-1 and JCt-1 data sets with the consensus values. The difference of Ba/Ca in JCp-1 between the means of our values prior to corrections for instrumental drift and the consensus values are almost the same as that in JCt-1, that is, falling along the 1:1 line (Figure 4a). In addition, our values of Ba/Ca in JCp-1 and JCt-1 prior to corrections for instrumental drift were similar to the interlaboratory results within the 95% confidence interval. Our calibration, which contains a stable offset of Ba/Ca from 3 to 12 μmol/mol (Figure 1c), allows us to correct the absolute values of Ba/Ca with little bias in the coral Ba/Ca range. We note that the consensus values of Ba/Ca ratio in JCt-1 and JCp-1 were defined from the analytical result using ICP-MS in 10 laboratories. Measuring Ba/Ca in JCp-1 and JCt-1 from more laboratories would improve the accuracy and precision of Ba/Ca analysis. For Sr/Ca, our values in JCp-1 and JCt-1 prior to corrections for instrumental drift were also similar to the interlaboratory work within the 95% confidence interval (Figure 4b). However, the difference of Sr/Ca in JCt-1 between the means of our values prior to corrections for instrumental drift and the consensus values is lower than that in JCp-1, that is, falling far from the 1:1 line (Figure 4b). This implies that a bias in the Sr/Ca value in JCt-1 may appear. However, it does not influence coral Sr/Ca analyses since the Sr/Ca in JCt-1 is much lower than the reported Sr/Ca range in coral skeletons (Figure 1d). The bias in Sr/Ca in JCt-1 may be caused by the values being out of our calibration range (Figure 1d). We note that the interlaboratory data using ICP-OES (Hathorne, Gagnon, et al., 2013) showed a negative correlation between the differences of Sr/Ca in JCp-1 and that in JCt-1 ($r = -0.82$; $p < 0.01$; $n = 9$; Figure 4b), which is not confirmed by our results.

15252027, 2021, 22, Downloaded from https://agupubs.onlinelibrary.wiley.com. By Hokkaido University- on [04/10/2021]. Re-use and distribution is strictly not permitted, except for Open Access articles

5. Conclusions

Our new method using ICP-OES combined with an ultrasonic nebulizer and intensity ratio calibration determines coral Ba/Ca and Sr/Ca at a Ca concentration of 9 ± 2 mg/L. The analytical precisions of Ba/Ca and Sr/Ca are within ±0.17 μmol/mol and ±0.026 mmol/mol (1 SD), respectively. The ultrasonic nebulizer is effective in improving the analytical signal of TE in coral skeletons. The influence of the high Ca concentrations on the coral Ba/Ca analysis is reduced by applying the intensity ratio calibration method and analyzing at a certain Ca concentration. Our new method to analyze coral Ba/Ca and Sr/Ca using ICP-OES will use for establishing the century-long coral record at monthly resolution, which significantly contributes to paleolimnology and paleoceanography, for example, reconstructions of monsoonal rainfall, river floods, coastal upwelling, and sea surface temperatures in recent centuries. Our new method using an ultrasonic nebulizer is expected to be applied to other coral skeletal proxies (e.g., Mg/Ca, supporting information, Li/Ca, and Mn/Ca; Fowell et al., 2016; Hathorne, Felis, et al., 2013; Montagna et al., 2014; Shen and Boyle, 1988; Thompson et al., 2015). Analyses of the multiple TEs would disentangle the complexity of coral skeletal proxies caused by their SST dependency and vital effect (Bryan et al., 2019; DeCarlo et al., 2016; Gaetani et al., 2011).

Conflict of Interest

All authors declare that they have no competing interest.

Data Availability Statement

All data is available on the data repository at KIKAI Institute for coral reef sciences (https://coralogy.kikaireefs.org/C-1%20Scientific%20data.html).

Acknowledgments
The authors thank Saori Ito, Taro Komagoe, and Tung Than Phan for providing the results of JCt-1 and JCp-1 data in their analyses. The authors are grateful for the support of Saori Ito and Yuri Sasaki, who assisted with ICP-OES management in the CREES laboratory.

References

Bryan, S. P., Hughen, K. A., Karnauskas, K. B., & Farrar, J. T. (2019). Two hundred fifty years of reconstructed South Asian summer monsoon intensity and decadal-scale variability. *Geophysical Research Letters*, *46*(7), 3927–3935. https://doi.org/10.1029/2018GL081593

Cantarero, S., Tl Tanzil, J., & Goodkin, N. F. (2017). Simultaneous analysis of Ba and Sr to Ca ratios in scleractinian corals by inductively coupled plasma optical emissions spectrometry. *Limnology and Oceanography: Methods*, *15*(1), 116–123. https://doi.org/10.1002/lom3.10152

DeCarlo, T. M., Gaetani, G. A., Cohen, A. L., Foster, G. L., Alpert, A. E., & Stewart, J. A. (2016). Coral Sr-U thermometry. *Paleoceanography*, *31*(6), 626–638. https://doi.org/10.1002/2015PA002908

de Villiers, S., Greaves, M., & Elderfield, H. (2002). An intensity ratio calibration method for the accurate determination of Mg/Ca and Sr/Ca of marine carbonates by ICP-AES. *Geochemistry, Geophysics, Geosystems*, *3*(1), a–n. https://doi.org/10.1029/2001GC000169

Fowell, S. E., Sandford, K., Stewart, J. A., Castillo, K. D., Ries, J. B., & Foster, G. L. (2016). Intrareef variations in Li/Mg and Sr/Ca sea surface temperature proxies in the Caribbean reef-building coral Siderastrea siderea. *Paleoceanography*, *31*(10), 1315–1329. https://doi.org/10.1002/2016PA002968

Gaetani, G. A., Cohen, A. L., Wang, Z., & Crusius, J. (2011). Rayleigh-based, multi-element coral thermometry: A biomineralization approach to developing climate proxies. *Geochimica et Cosmochimica Acta*, *75*(7), 1920–1932. https://doi.org/10.1016/j.gca.2011.01.010

Gonneea, M. E., Cohen, A. L., DeCarlo, T. M., & Charette, M. A. (2017). Relationship between water and aragonite barium concentrations in aquaria reared juvenile corals. *Geochimica et Cosmochimica Acta*, *209*, 123–134. https://doi.org/10.1016/j.gca.2017.04.006

Hathorne, E. C., Felis, T., Suzuki, A., Kawahata, H., & Cabioch, G. (2013). Lithium in the aragonite skeletons of massive Porites corals: A new tool to reconstruct tropical sea surface temperatures. *Paleoceanography*, *28*(1), 143–152. https://doi.org/10.1029/2012PA002311

Hathorne, E. C., Gagnon, A., Felis, T., Adkins, J., Asami, R., Boer, W., et al. (2013). Interlaboratory study for coral Sr/Ca and other element/Ca ratio measurements. *Geochemistry, Geophysics, Geosystems*, *14*(9), 3730–3750. https://doi.org/10.1002/ggge.20230

Hendy, E. J., Gagan, M. K., Alibert, C. A., McCulloch, M. T., Lough, J. M., & Isdale, P. J. (2002). Abrupt decrease in tropical Pacific Sea surface salinity at end of Little Ice Age. *Science*, *295*(5559), 1511–1514. https://doi.org/10.1126/science.1067693

Ito, S., Watanabe, T., Yano, M., & Watanabe, T. K. (2020). Influence of local industrial changes on reef coral calcification. *Scientific Reports*, *10*(1), 1–11. https://doi.org/10.1038/s41598-020-64877-6

LaVigne, M., Grottoli, A. G., Palardy, J. E., & Sherrell, R. M. (2016). Multi-colony calibrations of coral Ba/Ca with a contemporaneous in situ seawater barium record. *Geochimica et Cosmochimica Acta*, *179*, 203–216. https://doi.org/10.1016/j.gca.2015.12.038

Lea, D. W., Shen, G. T., & Boyle, E. A. (1989). Coralline barium records temporal variability in equatorial Pacific upwelling. *Nature*, *340*(6232), 373–376. https://doi.org/10.1038/340373a0

McCulloch, M., Fallon, S., Wyndham, T., Hendy, E., Lough, J., & Barnes, D. (2003). Coral record of increased sediment flux to the inner Great Barrier Reef since European settlement. *Nature*, *421*(6924), 727–730. https://doi.org/10.1038/nature01361

Montaggioni, L. F., Le, F., Corrège, T., & Cabioch, G. (2006). Coral barium/calcium record of mid-Holocene upwelling activity in New Caledonia, South-West Pacific. *Palaeogeography, Palaeoclimatology, Palaeoecology*, *237*, 436–455. https://doi.org/10.1016/j.palaeo.2005.12.018

Montagna, P., McCulloch, M., Douville, E., López Correa, M., Trotter, J., Rodolfo-Metalpa, R., et al. (2014). Li/Mg systematics in scleractinian corals: Calibration of the thermometer. *Geochimica et Cosmochimica Acta*, *132*, 288–310. https://doi.org/10.1016/j.gca.2014.02.005

Okai, T., Suzuki, A., Kawahata, H., Terashima, S., & Imai, N. (2002). Preparation of a New Geological Survey of Japan Geochemical Reference Material: Coral JCp-1. *Geostandards and Geoanalytical Research*, *26*(1), 95–99. https://doi.org/10.1111/j.1751-908X.2002.tb00627.x

Olson, K. W., Haas, W. J., & Fassel, V. A. (1977). Multielement detection limits and sample nebulization efficiencies of an improved ultrasonic nebulizer and a conventional pneumatic nebulizer in inductively coupled plasma-atomic emission spectrometry. *Analytical Chemistry*, *49*(4), 632–637. https://doi.org/10.1021/ac50012a032

Phan, T. T., Yamazaki, A., Chiang, H. W., Shen, C. C., Doan, L. D., & Watanabe, T. (2019). Mekong River discharge and the East Asian monsoon recorded by a coral geochemical record from Con Dao Island, Vietnam. *Geochemical Journal*, *53*(2), e1–e7. https://doi.org/10.2343/geochemj.2.0552

R Core Team. (2020). *R: A language and environment for statistical computing*. R Foundation for Statistical Computing. https://www.R-project.org/

Schrag, D. P. (1999). Rapid analysis of high-precision Sr/Ca ratios in corals and other marine carbonates. *Paleoceanography*, *14*(2), 97–102. https://doi.org/10.1029/1998PA900025

Shen, G. T., & Boyle, E. A. (1988). Determination of lead, cadmium and other trace metals in annually-banded corals. *Chemical Geology*, *67*(1–2), 47–62. https://doi.org/10.1016/0009-2541(88)90005-8

Sowa, K., Watanabe, T., Kan, H., & Yamano, H. (2014). Influence of Land Development on Holocene Porites Coral Calcification at Nagura Bay, Ishigaki Island, Japan. *PloS One*, *9*(2), e88790. https://doi.org/10.1371/journal.pone.0088790

Thompson, D. M., Cole, J. E., Shen, G. T., Tudhope, A. W., & Meehl, G. A. (2015). Early twentieth-century warming linked to tropical Pacific wind strength. *Nature Geoscience*, *8*(2), 117–121. https://doi.org/10.1038/ngeo2321

Tudhope, A. W., Lea, D. W., Shimmield, G. B., Chilcott, C. P., & Head, S. (1996). Monsoon climate and Arabian Sea castal upwelling recorded in massive corals from Southern Oman. *PALAIOS*, *11*(4), 347. https://doi.org/10.2307/3515245

Watanabe, T., Winter, A., & Oba, T. (2001). Seasonal changes in sea surface temperature and salinity during the Little Ice Age in the Caribbean Sea deduced from Mg/Ca and 18O/16O ratios in corals. *Marine Geology*, *173*(1–4), 21–35. https://doi.org/10.1016/S0025-3227(00)00166-3

Watanabe, T. K., Watanabe, T., Ohmori, K., & Yamazaki, A. (2020). Improving analytical method of Sr/Ca ratios in coral skeletons for paleo- SST reconstructions using ICP-OES. *Limnology and Oceanography: Methods*, *18*, 297–310. https://doi.org/10.1002/lom3.10357

Weldeab, S., Lea, D. W., Schneider, R. R., & Andersen, N. (2007). 155,000 years of West African monsoon and ocean thermal evolution. *Science*, *316*(5829), 1303–1307. https://doi.org/10.1126/science.1140461

Yamazaki, A., Yano, M., Harii, S., & Watanabe, T. (2020). Effects of light on the Ba/Ca ratios in coral skeletons. *Chemical Geology*, 119911. https://doi.org/10.1016/j.chemgeo.2020.119911

Yu, T. L., Wang, B. S., You, C. F., Burr, G. S., Chung, C. H., & Chen, Y. G. (2015). Geochemical effects of biomass burning and land degradation on Lanyu Islet, Taiwan. *Limnology & Oceanography*, *60*(2), 411–418. https://doi.org/10.1002/lno.10039

Zinke, J., Dullo, W.-C., Heiss, G. A., & Eisenhauer, A. (2004). ENSO and Indian Ocean subtropical dipole variability is recorded in a coral record off southwest Madagascar for the period 1659 to 1995. *Earth and Planetary Science Letters*, *228*(1–2), 177–194. https://doi.org/10.1016/j.epsl.2004.09.028

15252027, 2021, 22, Downloaded from https://agupubs.onlinelibrary.wiley.com. By Hokkaido University- on [04/10/2021]. Re-use and distribution is strictly not permitted, except for Open Access articles